Entanglement Properties and Quantum Phases for a Fermionic Disordered One-Dimensional Wire with Attractive Interactions

Richard Berkovits
Department of Physics, Jack and Pearl Resnick Institute, Bar-Ilan University, Ramat-Gan 52900, Israel
(Received 3 May 2015; published 9 November 2015)

A fermionic disordered one-dimensional wire in the presence of attractive interactions is known to have two distinct phases, a localized and superconducting, depending on the strength of interaction and disorder. The localized region may also exhibit a metallic behavior if the system size is shorter than the localization length. Here we show that the superconducting phase has a distribution of the entanglement entropy distinct from the metallic regime. The entanglement entropy distribution is strongly asymmetric with a Lévy α-stable distribution (compared to the Gaussian metallic distribution), as is seen also for the second Rényi entropy distribution. Thus, entanglement properties may reveal properties which cannot be detected by other methods.

DOI: 10.1103/PhysRevLett.115.206401 PACS numbers: 71.10.Pm, 03.65.Ud, 73.20.Fz, 73.21.Hb

In the last decade the application of concepts from quantum information, such as entanglement entropy (EE) [1], took center stage in understanding physical phenomena in condensed matter physics. One of the reasons for this interest is that EE is deeply connected to quantum phase transitions. The EE quantifies the entanglement in a many-body system by dividing it into two regions A and B. For a system in a pure state $|\Psi\rangle$, the entanglement between regions A and B is measured by the EE $S_{A\mathrm{or}B}$, related to the eigenvalues of the reduced density matrix of area A (ρ_A) or B (ρ_B). It is expected that nonlocal properties, such as the EE, may provide a different perspective beyond the traditional point-point correlations and local order parameters [2–11]. This is also very useful for numerical methods, such as the density matrix renormalization group (DMRG), which are ill suited for the calculation of a pair of operators in spatially distant locations as required for long-range correlations.

Specifically, ρ_A is defined as $\rho_A = \mathrm{Tr}_B|\Psi\rangle\langle\Psi|$, where the degrees of freedom of region B are traced out. The eigenvalues of the matrix λ_i^A are used to calculate the EE,

$$S_A = -\sum_i \lambda_i^A \ln \lambda_i^A, \tag{1}$$

and the Rényi entropy,

$$S_{nA} = -\frac{1}{1-n}\ln \sum_i (\lambda_i^A)^n, \tag{2}$$

where the first Rényi entropy ($n \to 1$) is equal to the EE $S_{1A} = S_A$. Thus the EE is the von Neumann (Shannon) entropy of λ_i^A, and the knowledge of the Rényi entropies for different n's probes the full spectrum of $\{\lambda_i^A\}$. For one-dimensional (1D) systems, the area of the boundary between regions A and B is fixed and thus the EE should not depend on the size of region A. Nevertheless, a logarithmic dependence of the form [12–15]:

$$S(L_A, L) = \frac{1}{6}\ln\left(\sin\left(\frac{\pi L_A}{L}\right)\right) + c, \tag{3}$$

where L_A is the length of region A and L is the sample's length, is expected in the metallic (clean) regime.

In this Letter we will use the EE and the second Rényi entropy (SRE) in order to investigate the nature of different phases of fermionic disordered 1D systems with attractive interactions. Electron-electron interactions in 1D systems are parametrized by the Luttinger parameter K [16,17]. For noninteracting systems $K = 1$, while for attractive interactions $K > 1$. When both disorder and interaction are present, an extended metallic (with superconducting correlations) phase is expected once attractive interactions are strong enough, i.e., $K > 1.5$ [17–20]. This stems from the renormalization group scaling of the localization length

$$\xi = (\xi_0)^{1/(3-2K)}, \tag{4}$$

where ξ_0 is the noninteracting localization length. Thus, for $K = 1.5$ the localization length diverges, and one transits from the localized to the extended regime. Indeed, it has been numerically demonstrated that with strong enough attractive interactions in the usual Anderson model [21–24] metal-like behavior emerges, although no evidence of superconducting correlation has been numerically demonstrated.

For disordered systems one must consider the EE behavior over an ensemble of different realizations of disorder. It has been demonstrated [25] that the median EE for $L_A < \xi$ follows the metallic logarithmic behavior [Eq. (3)], while for $L_A > \xi$ it saturates. In principle, this could be used to decide in what phase (localized or

metallic) the system is in [24]. Nevertheless, in a realistic numerical study this strategy is fraught with problems, since the localization length grows rapidly as a function of K [Eq. (4)], and easily outgrows any finite system length L. Once $\xi \gg L$ a finite system will show metallic behavior although it is in the localized regime. For brevity, we shall refer to the $K > 1.5$ regime as superconducting, and to the finite sample $K < 1.5$ regime as localized or metallic according to whether $L > \xi$ or $\xi > L$.

In this Letter we will show that the full distribution of the EE shows different behaviors in the metallic and superconducting regimes, although the median EE is essentially identical in both regimes. The EE distribution changes from a Gaussian in the metallic regime to a very asymmetric Lévy α-stable distribution (LASD) with "fat tails" in the superconducting regime. This behavior gives us a convenient numerical way to identify the phase of a system. Moreover, since an asymmetric LASD is also seen for the SRE distribution, it could also be measured experimentally. Thus, the EE and the SRE distributions are able to characterize the phase of the system, where other methods fail.

In this Letter we consider a 1D wire of length L populated by spinless electrons with *attractive* nearest-neighbor interactions and on-site disordered potential. The system's Hamiltonian is given by

$$H = \sum_{j=1}^{L} \epsilon_j \hat{c}_j^\dagger \hat{c}_j - t \sum_{j=1}^{L-1} (\hat{c}_j^\dagger \hat{c}_{j+1} + \text{H.c.}) + U \sum_{j=1}^{L-1} \left(\hat{c}_j^\dagger \hat{c}_j - \frac{1}{2}\right)\left(\hat{c}_{j+1}^\dagger \hat{c}_{j+1} - \frac{1}{2}\right), \quad (5)$$

where ϵ_j is the on-site energy, which is drawn from a uniform distribution $[-W/2, W/2]$, $\hat{c}_j^\dagger$ is the creation operator for a spinless electron at site j, and $t = 1$ is the hopping matrix element. The interaction strength is $U < 0$, and a background is included. For the noninteracting Anderson model the system is localized with a localization length $\xi_0 \approx 105/W^2$ [26]. Here the Luttinger parameter $K(U) = \pi/[2\cos^{-1}(-U/2)]$ [27,28]. For noninteracting electrons $K(U = 0) = 1$. For attractive interactions $K > 1$ and ξ increases as U becomes more negative. For $U = -1$, $K = 1.5$ and the localization length according to Eq. (4) diverges. Thus, below $U < -1$ the system is expected to be delocalized. At $U = -2$ it goes through another phase transition to a phase separated state and is insulating again. Indeed, numerically [21–24], this system is known to exhibit extended behavior for a range of attractive interaction strength centered around $U = -1.5$ and not too strong disorder $W < 1.5$.

The DMRG [29,30] is a very accurate numerical method for calculating the ground state of the disordered interacting 1D system and for the calculation of the reduced density matrix. We calculate the EE for three lengths $L = 300, 700, 1100$ and different values of $L_A = 10, 20, \ldots, L - 10$, for 400, 200, 100 realizations of disorder for the corresponding system length. Specifically, we calculate the normalized EE of the jth realization at a given L_A, $s_j(L_A) = S_j(L_A)/\langle S(L_A)\rangle$, where $\langle S(L_A)\rangle$ is the average EE over the different realizations. Since the distribution of the EE is very similar for different values of L_A as long as L_A is not too close to the edge we accumulate the distribution of the normalized EE, $P(s)$, in the range of $L/4 < L_A < 3L/4$.

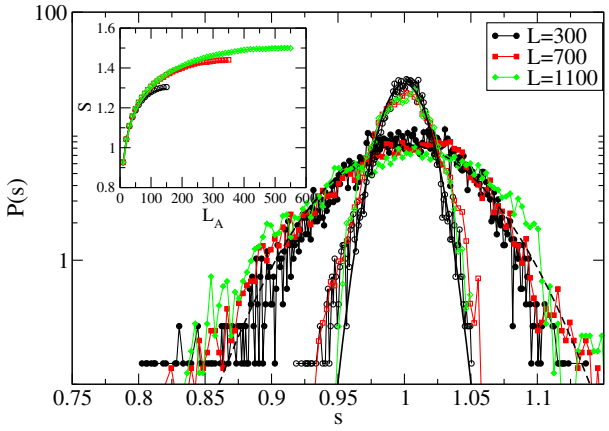

FIG. 1 (color online). The distribution $P(s)$ of the normalized EE (see text) for different length $L = 300$ (black, circles), $L = 700$ (red, squares), $L = 1100$ (green, diamonds), and disorder strength $W = 0.3$ (open symbols), $W = 0.7$ (closed symbols). A fit to a Gaussian with a width which depends on the disorder $\sigma(W)$ is depicted by the continuous lines. (Inset) The median EE as function of L_A. The symbols correspond to the numerical results, the curves to Eq. (3).

Let us begin by discussing the EE distribution for $U = -0.7$ [$K(U = -0.7) = 1.3$] for which the system is in the metallic regime, i.e., for localization lengths much larger than sample length. In Fig. 1 we present the distribution for two values of disorder ($W = 0.3, W = 0.7$), corresponding to the noninteracting localization length $\xi_0(W = 0.3) \sim 1200$ and $\xi_0(W = 0.7) \sim 200$, thus $\xi(W = 0.3, U = -0.7) \sim 5 \times 10^7$, and $\xi(W = 0.7, U = -0.7) \sim 6 \times 10^5$. First, we examine the median value of the EE as function of L_A (here we could use the average which is almost equal to the median, but for the sake of uniformity with the upcoming results we use here the median) and compare it with the expression of the EE for a clean system described in Eq. (3). As can be seen in the inset of Fig. 1 it fits quite well. Thus, the median EE follows closely the expected behavior of a clean (metallic) system. The distribution $P(s)$ for all three length and two disorder strength is plotted in Fig. 1. As has been discussed in Ref. [31], for $L \ll \xi$, we expect the distribution to be Gaussian, i.e., $(\sqrt{2\pi}\sigma)^{-1} \exp[-(s-\mu)^2/2\sigma^2]$, centered at the average μ. This is indeed seen in Fig. 1 (up to a slight skewness of the tails), as well as the fact that the width, σ of the Gaussian is almost independent of L. On the other hand, it is clear that

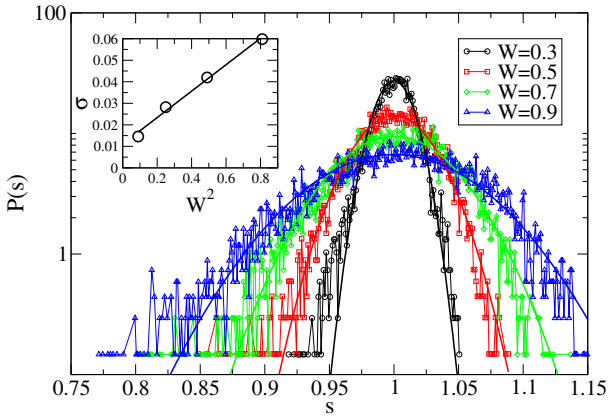

FIG. 2 (color online). The distribution $P(s)$ of the normalized EE for a fixed wire length ($L = 300$) and different disorder strength: $W = 0.3$ (black circles), $W = 0.5$ (red squares), $W = 0.7$ (green diamonds), $W = 0.9$ (blue triangles). A fit to a Gaussian of width $\sigma(W)$ (depicted in the inset) is indicated by the continuous lines. (Inset) The Gaussian width σ as a function of the disordered strength square W^2.

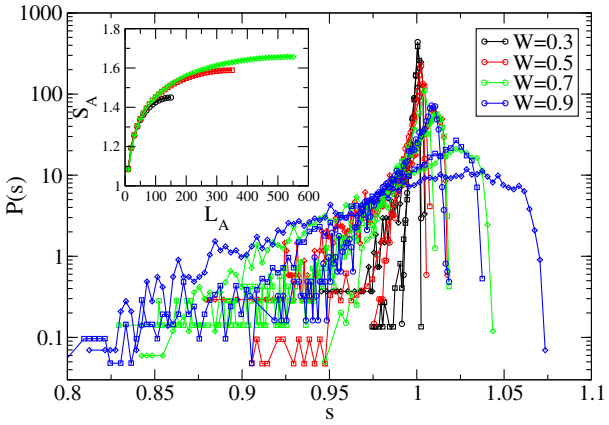

FIG. 3 (color online). The distribution $P(s)$ of the normalized EE deep in the superconducting regime ($U = -1.5$) for different strength of disorder ($W = 0.3$, black; $W = 0.5$, red; $W = 0.7$, green; $W = 0.9$, blue symbols) and sample length $L = 300$ (circles), $L = 700$ (squares), $L = 1100$ (diamonds). (Inset) The median EE as a function of L_A. The symbols correspond to the numerical results, the curves to Eq. (3).

the disorder strength W does affect σ. As expected, the weaker the disorder, the narrower is the width of the Gaussian.

The dependence of the Gaussian width on W is examined in Fig. 2. We keep the length and interaction strength fixed ($L = 300$, $U = -0.7$) while varying W. Even for the strongest disorder $\xi(W = 0.9, U = -0.7) \sim 2 \times 10^5$, is much larger than the sample length. $P(s)$ remains Gaussian for all disorder strength. Moreover, as can be seen from the inset $\sigma(W) \propto W^2$.

What happens to the EE distribution in the superconducting regime? Specifically, we concentrate on the extended regime with $U = -1.5$ ($K(U = -1.5) = 2.3$), different values of disorder $W = 0.3$, 0.5, 0.7, 0.9 corresponding to a non-interacting mean free path $\xi_0 \sim 1200$, 400, 200, 130 and different sample lengths $L = 300$, 700, 1100. This regime of the parameter space is deep in the superconducting regime. We present the distribution $P(s)$ for all lengths and interaction strengths in Fig. 3. It is obvious that $P(s)$ is completely different than in the metallic regime (Figs. 1 and 2). In all cases the distribution is strongly asymmetric. The median value of the EE is close to its maximum value, and the probability of measuring an EE larger than the median is rather small and falls off abruptly. On the other hand, there is a high probability for measuring values of the EE much below the median value. For smaller values of the EE the distribution has a very long tail. Another difference is the strong dependence on the sample length L even at the same value of disorder W.

First, one concludes that similarly to the case of a localized system ($L > \xi$) [25,31,32], the average EE is not a correct description of the superconducting regime typical EE. The EE is more appropriately represented by the median. In the inset of Fig. 3 the median of the EE as function of L_A is compared to Eq. (3), and fits quite well.

As can be seen in Fig. 4, the distribution is universal and may be scaled by the function $\tilde{P}(u)$, here $u = 1 + (s - 1)P_{\max}$, and the distribution is normalized $\tilde{P}(u) = P(u)/P_{\max}$, where $P_{\max}$ is the value of $P(s)$ at the maximum. In the inset of Fig. 4, the values of $P_{\max}$ vs ξ_0/L is depicted. Up to the ballistic regime, i.e., for $\xi_0 \gg L$, a linear relation seems to hold. The distribution $\tilde{P}(u)$ may be described rather well by a LASD, which is a natural extension of the central limit theorem for the case where the identically distributed random variables have no finite

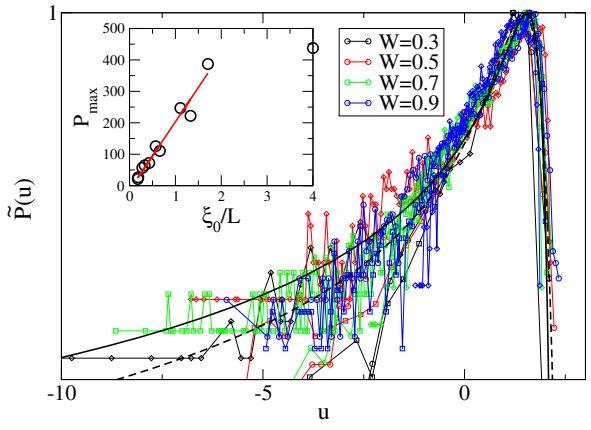

FIG. 4 (color online). The data presented in Fig. 3 scaled by the parameter u (see text). The continuous (dashed) black curve is the LASD with $\alpha = 1$, $\beta = -1$, $\gamma = 0.285$, $\delta = 0.8$, ($\alpha = 1.2$, $\beta = -1$, $\gamma = 0.28$, $\delta = 0.52$). (Inset) The maximum of the distribution $P(s)$ ($P_{\max}$) depicted in Fig. 3 as a function of ξ_0/L. A linear behavior in the regime $\xi_0/L < 2$ is indicated by the line.

variance, and is used to describe distributions with fat tails. The LASD [33–35]

$$f(x,\alpha,\beta,\gamma,\delta)=\frac{1}{\pi}\mathrm{Re}\int_0^\infty e^{it(x-\mu)}e^{-(\gamma t)^\alpha(1-i\beta\Phi)}dt, \quad (6)$$

[where $\Phi=\tan(\pi\alpha/2)$, except for $\alpha=1$ where $\Phi=-(2/\pi)\log(t)$], is defined by four parameters. The stability index $0\le\alpha<2$ characterizes the asymptotic behavior of the tails $|x|^{-1-\alpha}$ (except for $\alpha=2$), the skewness parameter $-1\le\beta\le1$, γ is a scale factor and δ controls the location of the maximum [33]. In general f is not known analytically, except for special cases, such as $f(x,\alpha=2,\beta,\gamma=\sigma/\sqrt{2},\delta=\bar{x})$, equal to a Gaussian of width σ. We plot $f(u,\alpha=1,\beta=-1,\gamma=0.285,\delta=0.8)$, and $f(u,\alpha=1.2,\beta=-1,\gamma=0.28,\delta=0.52)$ in Fig. 4. The skewness is clearly maximal ($\beta=-1$), while fitting α depends very much on the tail region, which has the largest numerical uncertainty. Nevertheless, the main part of the distribution is evidently fitted well by $1<\alpha<1.2$.

Thus, although the median of the EE (or its average) does not give us a clear signature whether the system is in the metallic regime or in the superconducting one, the distribution can differentiate between the regimes. Further work is needed in order to follow how the distribution changes as one goes through the phase transition and whether the transition point is characterized by a special distribution. A hint may be found in Ref. [24], where the variance of the EE is plotted through the transition. It seems that the variance becomes smaller in the metallic side as one approaches the transition and then grows again in the superconducting regime. This is in line with a crossover from a Gaussian distribution to a fat tail one.

One of the earliest suggestions for an experimental measure of the EE is the current noise [2,36]. This is based on a connection between the fluctuations in the number of particles measured in region A (i.e., the full counting statistics) and the EE. Nevertheless, it has been shown to fail for interacting systems [37]. In Fig. 3(a) we probe the distribution of the fluctuations in the number of particles in region A, $\delta N_A=N_A-\langle N_A\rangle$. It is clear that the distribution of δN_A is wider in the superconducting phase. This is in line with the correspondence between δN_A and EE. On the other hand, the distribution of δN_A remains Gaussian, with no signature of significant fat tails. Thus, the current noise does not carry any distinct signatures of the EE distribution.

A more direct way to measure the entanglement is through the measurement of the SRE [Eq. (2), $n=2$], which measures the overlap between the ground state of two identical copies of a system when region A is swapped between them [38,39]. There are suggestions for experimentally measuring the SRE through coupling between two identical copies of cold atoms in optical lattices [40–42]. Thus, a direct evaluation of the distribution of

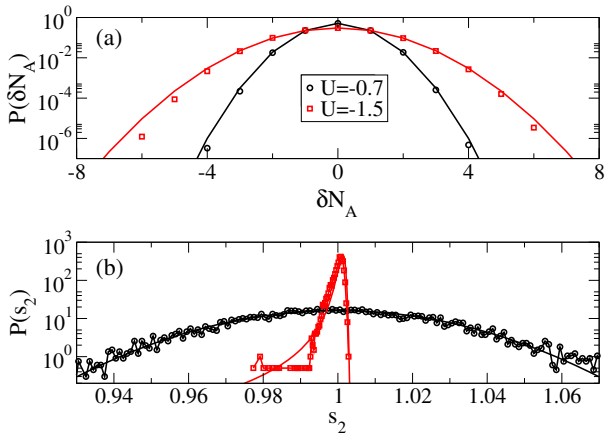

FIG. 5 (color online). (a) The distribution of δN_A, for the metallic ($U=-0.7$, black circles) and superconducting ($U=-1.5$, red squares) regimes for $L=700$ and $W=0.3$. The black (red) line corresponds to a fit to a Gaussian distribution with $\sigma=0.78$ ($\sigma=1.32$). (b) The distribution of the SRE, $P(s_2)$, for the two phases. In the metallic regime the distribution fits a Gaussian with width $\sigma=2.5\times10^{-2}$ (black line). For the superconducting regime a fit to the LASD with $\alpha=1.3,\beta=-1$, $\gamma=6\times10^{-4},\delta=1$ (red line).

S_{2A} is of interest. As can be seen in Fig. 5(b), the distribution of $P(s_2)$ (calculated in the same way as for the EE), shows similar differences between metallic and superconducting behavior, i.e., Gaussian vs LASD behavior.

What stands behind the EE distribution in the superconducting phase? The phase and number operator are canonically conjugate, and since in the superconducting regime the phase is constant, the number fluctuations should grow compared to the metallic one, as can be seen by direct calculation [Fig. 5(a)]. Nevertheless, EE reveals information beyond the number fluctuations. The fat tail distribution may be explained by the following picture: One might think of the disordered superconducting state as regions of superconducting phase of random sizes, connected by weak links. This picture leads to a broad distribution of the EE due to the broad distribution of numbers and strength of links. In a sense, this is a mirror (dual) picture of the strongly localized regime, where a wide distribution of many physical quantities is seen.

To conclude, the EE and SRE distributions show a distinct behavior, depending if the system is in a metallic (system length much smaller than the localization length) or a superconducting (localization length diverges) regime. While the metallic regime shows a Gaussian distribution of the EE and SRE, the superconducting EE and SRE shows an asymmetric distribution. Thus, the entanglement properties encode details of the underlying phase of the system which may elude other measures, useful for detecting new phases both numerically and experimentally. The

emergence of a fat tail distribution for the EE and SRE in the superconducting regime is fascinating and deserves further study.

I would like to thank B. Altshuler, I. Aleiner, and V. Oganesyan, for useful discussions. Financial support from the Israel Science Foundation (Grant No. 686/10) is gratefully acknowledged.

[1] For recent reviews, see L. Amico, R. Fazio, A. Osterloh, and V. Vedral, Rev. Mod. Phys. **80**, 517 (2008); J. Eisert, M. Cramer, and M. B. Plenio, Rev. Mod. Phys. **82**, 277 (2010), and references therein.
[2] H. F. Song, S. Rachel, C. Flindt, I. Klich, N. Laflorencie, and K. Le Hur, Phys. Rev. B **85**, 035409 (2012).
[3] Z.-C. Gu and X.-G. Wen, Phys. Rev. B **80**, 155131 (2009).
[4] R. Horodecki, P. Horodecki, M. Horodecki, and K. Horodecki, Rev. Mod. Phys. **81**, 865 (2009).
[5] O. Gühne and G. Tóth, Phys. Rep. **474**, 1 (2009).
[6] F. Franchini, J. Cui, L. Amico, H. Fan, M. Gu, V. Korepin, L. C. Kwek, and V. Vedral, Phys. Rev. X **4**, 041028 (2014).
[7] T. J. Osborne and M. A. Nielsen, Phys. Rev. A **66**, 032110 (2002).
[8] S.-J. Gu, S.-S. Deng, Y.-Q. Li, and H.-Q. Lin, Phys. Rev. Lett. **93**, 086402 (2004).
[9] J. I. Latorre and A. Riera, J. Phys. A **42**, 504002 (2009).
[10] I. Affleck, N. Laflorencie, and E. S. Sorensen, J. Phys. A **42**, 504009 (2009).
[11] G. Refael and J. E. Moore, J. Phys. A **42**, 504010 (2009).
[12] C. Holzhey, F. Larsen, and F. Wilczek, Nucl. Phys. **B424**, 443 (1994).
[13] G. Vidal, J. I. Latorre, E. Rico, and A. Kitaev, Phys. Rev. Lett. **90**, 227902 (2003); J. I. Latorre, E. Rico, and G. Vidal, Quantum Inf. Comput. **4**, 048 (2004).
[14] P. Calabrese and J. Cardy, J. Stat. Mech. P06002 (2004).
[15] V. E. Korepin, Phys. Rev. Lett. **92**, 096402 (2004).
[16] W. Apel, J. Phys. C **15**, 1973 (1982); W. Apel and T. M. Rice, Phys. Rev. B **26**, 7063 (1982).
[17] T. Giamarchi and H. J. Schulz, Phys. Rev. B **37**, 325 (1988).
[18] C. L. Kane and M. P. A. Fisher, Phys. Rev. B **56**, 15231 (1997).
[19] I. V. Gornyi, A. D. Mirlin, and D. G. Polyakov, Phys. Rev. B **75**, 085421 (2007).
[20] M. P. A. Fisher and L. I. Glazmann, *Transport in One-Dimensional Luttinger Liquid* in *Mesoscopic Transport Theory*, NATO ASI Series E, edited by L. Sohn, L. P. Kouwenhoven, and G. Schön (Kluwer, Amsterdam, 1997), Vol. 345, p. 331.
[21] P. Schmitteckert, T. Schulze, C. Schuster, P. Schwab, and U. Eckern, Phys. Rev. Lett. **80**, 560 (1998); P. Schmitteckert, R. A. Jalabert, D. Weinmann, and J. L. Pichard, Phys. Rev. Lett. **81**, 2308 (1998).
[22] C. Schuster, R. A. Römer, and M. Schreiber, Phys. Rev. B **65**, 115114 (2002).
[23] J. M. Carter and A. MacKinnon, Phys. Rev. B **72**, 024208 (2005).
[24] A. Zhao, R.-L. Chu, and S.-Q. Shen, Phys. Rev. B **87**, 205140 (2013).
[25] R. Berkovits, Phys. Rev. Lett. **108**, 176803 (2012).
[26] R. A. Römer and M. Schreiber, Phys. Rev. Lett. **78**, 515 (1997).
[27] F. Woynarovich and H. P. Eckle, J. Phys. A **20**, L97 (1987); C. J. Hamer, G. R. W. Quispel, and M. T. Batchelor, *ibid.* **20**, 5677 (1987).
[28] T. Giamarchi, *Quantum Physics in One Dimension* (Oxford University Press, New York, 2003).
[29] S. R. White, Phys. Rev. Lett. **69**, 2863 (1992); Phys. Rev. B **48**, 10345 (1993).
[30] U. Schollwöck, Rev. Mod. Phys. **77**, 259 (2005); K. A. Hallberg, Adv. Phys. **55**, 477 (2006).
[31] R. Berkovits, J. Phys. Conf. Ser., **376**, 012020 (2012).
[32] R. Berkovits, Phys. Rev. B **89**, 205137 (2014).
[33] K. Burnecki, A. Wylomańska, A. Beletskii, V. Gonchar, and A. Chechkin, Phys. Rev. E **85**, 056711 (2012), and references therein.
[34] P. P. Lévy, *Calcul des Probabilités* (Gauthier Villars, Paris, 1925); *Théorie del'addition des Variables Aléatoires*, 2nd ed. (Gauthier Villars, Paris, 1937).
[35] B. V. Gnedenko and A. N. Kolmogorov, *Limit Distributions of Sums of Independent Random Variables* (Addison-Wesley, Cambridge, 1954).
[36] I. Klich and L. Levitov, Phys. Rev. Lett. **102**, 100502 (2009).
[37] B. Hsu, E. Grosfeld, and E. Fradkin, Phys. Rev. B **80**, 235412 (2009).
[38] P. Zanardi, C. Zalka, and L. Faoro, Phys. Rev. A **62**, 030301 (R) (2000).
[39] P. Horodecki and A. Ekert, Phys. Rev. Lett. **89**, 127902 (2002).
[40] D. A. Abanin and E. Demler, Phys. Rev. Lett. **109**, 020504 (2012).
[41] A. J. Daley, H. Pichler, J. Schachenmayer, and P. Zoller, Phys. Rev. Lett. **109**, 020505 (2012).
[42] R. Islam, R. Ma, P. M. Preiss, M. E. Tai, A. Lukin, M. Rispoli, and M. Greiner, arXiv:1509.01160.